






Article

Hadron-Induced Radiation Damage in Fast Heavy Inorganic Scintillators

Chen Hu ¹, Fan Yang ^{1,2}, Liyuan Zhang ¹, Ren-Yuan Zhu ^{1,*}, Jon Kapustinsky ³, Xuan Li ³, Michael Mocko ³, Ron Nelson ³, Steve Wender ³ and Zhehui Wang ³

¹ High Energy Physics, California Institute of Technology, Pasadena, CA 91125, USA

² School of Physics, Nankai University, Tianjin 300071, China

³ Los Alamos National Laboratory, Los Alamos, NM 87545, USA

* Correspondence: zhu@caltech.edu

Abstract: Fast and heavy inorganic scintillators with suitable radiation tolerance are required to face the challenges presented at future hadron colliders of high energy and intensity. Up to 5 GGy and 5×10^{18} n_{eq}/cm² of one-MeV-equivalent neutron fluence is expected by the forward calorimeter at the Future Hadron Circular Collider. This paper reports the results of an investigation of proton- and neutron-induced radiation damage in various fast and heavy inorganic scintillators, such as LYSO:Ce crystals, LuAG:Ce ceramics, and BaF₂ crystals. The experiments were carried out at the Blue Room with 800 MeV proton fluence up to 3.0×10^{15} p/cm² and at the East Port with one MeV equivalent neutron fluence up to 9.2×10^{15} n_{eq}/cm², respectively, at the Los Alamos Neutron Science Center. Experiments were also carried out at the CERN PS-IRRAD proton facility with 24 GeV proton fluence up to 8.2×10^{15} p/cm². Research and development will continue to develop LuAG:Ce ceramics and BaF₂:Y crystals with improved optical quality, F/T ratio, and radiation hardness.



Citation: Hu, C.; Yang, F.; Zhang, L.; Zhu, R.-Y.; Kapustinsky, J.; Li, X.; Mocko, M.; Nelson, R.; Wender, S.; Wang, Z. Hadron-Induced Radiation Damage in Fast Heavy Inorganic Scintillators. *Instruments* **2022**, *6*, 57. <https://doi.org/10.3390/instruments6040057>

Academic Editors: Fabrizio Salvatore, Alessandro Cerri, Antonella De Santo and Iacopo Vivarelli

Received: 10 August 2022

Accepted: 15 September 2022

Published: 5 October 2022

Publisher's Note: MDPI stays neutral with regard to jurisdictional claims in published maps and institutional affiliations.



Copyright: © 2022 by the authors. Licensee MDPI, Basel, Switzerland. This article is an open access article distributed under the terms and conditions of the Creative Commons Attribution (CC BY) license (<https://creativecommons.org/licenses/by/4.0/>).

Keywords: radiation hardness; irradiation; crystals; scintillators; protons; neutrons

1. Introduction

Future high-energy physics (HEP) experiments face an unprecedented challenge of a harsh radiation environment against ionization dose charged hadrons as well as neutral hadrons. The radiation environment expected by the forward calorimeter in the proposed Future Hadron Circular Collider (FCC-*hh*) reaches an ionization dose up to 5 GGy and a neutron fluence up to 5×10^{18} one-MeV-equivalent n_{eq}/cm² [1]. Bright and fast cerium-doped lutetium yttrium oxyorthosilicate (Lu_{2(1-x)}Y_{2x}SiO₅:Ce or LYSO:Ce) features high stopping power and suitable radiation tolerance against both ionization dose and hadrons. Under construction is the barrel timing layer (BTL) [2] using LYSO crystals for the compact muon solenoid (CMS) upgrade at the high-luminosity large hadron collider (HL-LHC). LYSO crystals were also proposed for the Mu2e experiment at Fermilab [3]. In addition, a total absorption LYSO calorimeter for the coherent muon to electron transition (COMET) experiment at the High-Energy Accelerator Research Organization (KEK) [4] and a 3D imaging calorimeter for the high-energy cosmic-radiation detection (HERD) experiment in space [5] are being built. Under investigation are cost-effective cerium-doped lutetium aluminum garnet (Lu₃Al₅O₁₂:Ce or LuAG:Ce) ceramics for the precision-timing, ultracompact, radiation-hard electromagnetic calorimetry (RADICAL) concept for future HEP experiments [6]. BaF₂ crystals also attract attention due to their ultrafast light with 0.5 ns decay time, which is considered for the Mu2e-II upgrade [7]. While radiation damage in fast and heavy inorganic scintillators against ionization dose is well understood [8–14], investigations are still ongoing to understand radiation damage against hadrons, including both charged hadrons [8,10,13–28] and neutrons [29–33].

Starting in 2014, a series of experiments was performed to study radiation damage in fast and heavy inorganic scintillators against hadrons by using 800 MeV protons at

the Blue Room and neutrons at the East Port, respectively, at the Los Alamos Neutron Science Center (LANSCE). Inorganic scintillators were irradiated up to 3.0×10^{15} p/cm² and 9.2×10^{15} one MeV equivalent n_{eq} /cm². LYSO:Ce crystals and LuAG:Ce ceramics were also irradiated at the European Organization for Nuclear Research (CERN) PS-IRRAD proton facility by 24 GeV protons up to 8.2×10^{15} p/cm². In this paper, we summarize our results obtained for LYSO:Ce crystals, LuAG:Ce ceramics, and BaF₂ crystals. The result of this work is of great importance for the CMS phase-II upgrade of the BTL detector [2] at the HL-LHC, as well as an ultra-radiation-hard RADICAL calorimetry [6] for the proposed FCC-hh.

2. Materials and Methods

The samples were produced at the Beijing Glass Research Institute (BGRI), the Beijing Opto-Electronics Technology Company Ltd. (BOET or OET), the Shanghai Institute of Ceramics (SIC), the Shanghai Institute of Optics and Fine Mechanics (SIOM), the Chongqing Shengpu Electronics Co. LTD (SIPAT), and the Sichuan Tianle Photonics Company (Tianle). Four proton irradiation experiments 6501 [25–27], 6990 [25–27], 7324 [28,33] and 8051 [33] were conducted in 2014, 2015, 2016, and 2018, respectively. Three neutron irradiation experiments 6991 [31,32], 7332 [31,32] and 7638 [31–33] were conducted in 2015, 2016, and 2017, respectively. Some LYSO:Ce and LuAG:Ce samples were also irradiated at the CERN PS-IRRAD facility. The details of these experiments and samples are listed in Table 1.

Table 1. Samples used in various proton and neutron irradiation experiments.

Experiment	Samples	Dimension (mm ³)	Fluence (cm ⁻²)
CERN PS-IRRAD	4 × SIC LYSO	14 × 14 × 1.5	7.4×10^{13} – 6.9×10^{15}
	10 × BOET LFS	14 × 14 × 1.5	1.0×10^{14} – 8.2×10^{15}
	2 × SIC LuAG	Φ14.4 × 1	7.1×10^{13} – 1.2×10^{15}
LANSCE-p-6990	OET LFS	25 × 25 × 180	1.8×10^{14} – 2.9×10^{15}
LANSCE-p-7324	SIC LYSO	25 × 25 × 200	5.0×10^{13} – 3.0×10^{15}
	9 × SIC LYSO	10 × 10 × 3	2.7×10^{13} – 9.7×10^{14}
	6 × SIC BaF ₂	25 × 25 × 5	2.7×10^{13} – 9.7×10^{14}
	6 × SIC PWO	25 × 25 × 5	2.7×10^{13} – 9.7×10^{14}
LANSCE-p-8051	SIPAT LYSO	25 × 25 × 200	3.8×10^{13} – 1.6×10^{15}
	Tianle LYSO	25 × 25 × 200	2.2×10^{13} – 1.8×10^{15}
LANSCE-n-6991	18 × OET LFS	14 × 14 × 1.5	9.4×10^{14} – 9.2×10^{15}
LANSCE-n-7332	12 × SIC LYSO	10 × 10 × 5	1.7×10^{15} – 8.3×10^{15}
	12 × SIC BaF ₂	15 × 15 × 5	1.7×10^{15} – 8.3×10^{15}
	12 × SIC PWO	15 × 15 × 5	1.7×10^{15} – 8.3×10^{15}
LANSCE-n-7638	6 × SIC LYSO	10 × 10 × 3	1.7×10^{15} – 6.7×10^{15}
	6 × Tianle LYSO	10 × 10 × 3	1.7×10^{15} – 6.7×10^{15}
	8 × BGRI BaF ₂	10 × 10 × 2	1.7×10^{15} – 6.7×10^{15}
	8 × SIC BaF ₂	10 × 10 × 2	1.7×10^{15} – 6.7×10^{15}
	3 × SIC LuAG	Φ14.4 × 1	1.7×10^{15} – 6.7×10^{15}

The LANSCE 800 MeV and the CERN PS-IRRAD 24-GeV proton beam show a Gaussian shape with a full width at half-maximum (FWHM) of about 25 and 12 mm, respectively. Dosimeters with a cross-section of 10 × 10 and 20 × 20 mm² were used to measure the proton fluence at CERN PS-IRRAD. The proton fluence at LANSCE was calculated by measuring the proton current. The systematic uncertainties of the proton fluence at CERN and LANSCE are 7% and 10%, respectively. In the neutron irradiation experiments, half of the samples used in experiments 7332 and 7638 were irradiated with a 5 mm lead shielding, the other half without lead shielding. The error for the neutron fluence is about 10%.

To avoid optical bleaching and thermal annealing, all samples were wrapped with aluminum foil during and after irradiation and were kept at room temperature after

irradiation. Transmittance was measured by using a Hitachi U3210 spectrophotometer with a precision of 0.2%. The emission-weighted longitudinal transmittance (*EWLT*) was calculated by using the equation

$$EWLT = \frac{\int T(\lambda)E_m(\lambda)d\lambda}{\int E_m(\lambda)d\lambda}, \quad (1)$$

where $T(\lambda)$ and $E_m(\lambda)$ are the transmittance and emission spectra, respectively. The *EWLT* is a numerical value of transmittance over the entire emission spectrum. The radiation-induced absorption coefficient (*RIAC*) was obtained from

$$RIAC = \frac{1}{l} \ln\left(\frac{T_0}{T_1}\right), \quad (2)$$

where l is the crystal length and T_0 and T_1 are the transmittances before and after irradiation, respectively.

The errors for the *RIAC* value depend on the light path length and the initial transmittance of the sample. For samples with suitable initial transparency, the errors are about 1, 3.5, and 5 m^{-1} for the thickness of 5, 1.5, and 1 mm, respectively. The *RIAC* errors for some LuAG:Ce ceramic samples could be larger than 5 m^{-1} because of poor initial transparency due to rough surfaces or scattering centers in the ceramic bulk [33]. A Hamamatsu R2059 PMT was used to measure the light output (LO) before and after irradiation with a grease coupling for 0.511-MeV γ -rays from a ^{22}Na source with a coincidence trigger. The uncertainty for the light output measurements is about 1%.

3. Results and Discussion

Figure 1 shows transmittance spectra for LYSO (top), BaF₂ (middle) and PWO crystals (bottom) measured before (black lines) and after (red lines) (a) proton irradiation with a proton fluence of 9.7×10^{14} p/cm² and (b) neutron irradiation [31,32] with a one-MeV-equivalent neutron fluence of 8.3×10^{15} n_{eq}/cm², respectively. Also shown in the figure are the emission spectra (blue dash lines), the numerical values of the *EWLT*, and the theoretical limit of transmittance (black dots) calculated according to the refractive index, assuming multiple bounces without internal absorption [34]. The results demonstrate that the radiation hardness of LYSO and BaF₂ crystals is much better than PWO crystals against both protons and neutrons.

Figure 2 shows LO as a function of integration time for LYSO (top), BaF₂ (middle), and PWO crystals (bottom) measured before (black) and after (red) (a) a proton fluence of up to 9.7×10^{14} p/cm² [28] and (b) a one MeV equivalent neutron fluence of up to 8.3×10^{15} n_{eq}/cm² [31,32], respectively. Also shown in the figure are the numerical values of LO (200), LO (2500), A₀, A₁, and τ , which represent the light output integrated into the time gate of 200 ns and 2500 ns, the fast component (if applicable), the slow component, and the decay time from the exponential fit. Since the light output of PWO crystals is too low after 9.7×10^{14} p/cm² and 8.3×10^{15} n_{eq}/cm², the data after 1.6×10^{14} p/cm² and 3.7×10^{15} n_{eq}/cm² are shown for PWO samples. We note that more than 91% and 77% LO remain for LYSO and BaF₂ crystals after 9.7×10^{14} p/cm² and 8.3×10^{15} n_{eq}/cm², respectively. This indicates that LYSO and BaF₂ crystals survive up to these hadron fluences but not PWO.

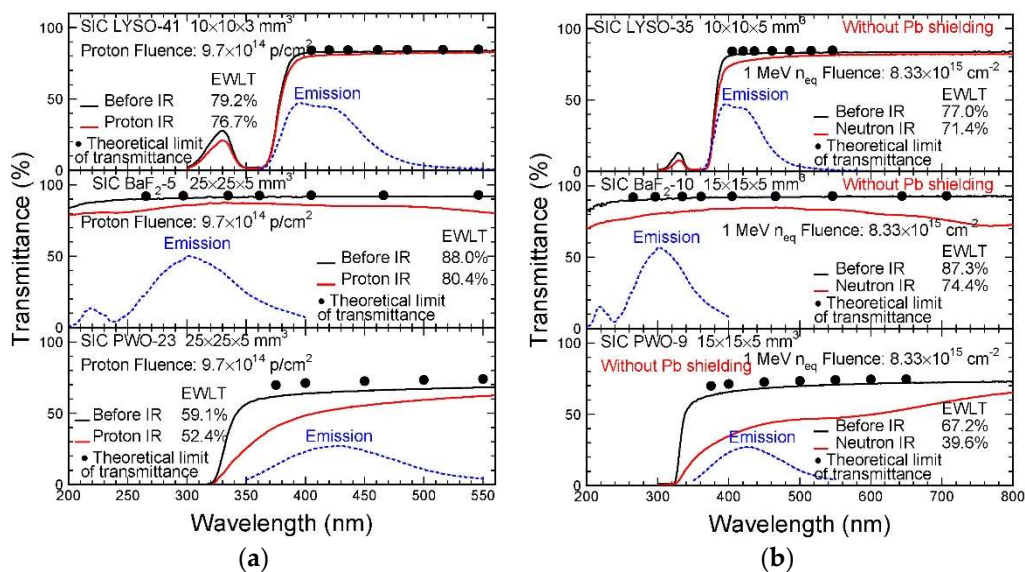


Figure 1. The transmittance spectra measured before (black lines) and after (red lines) irradiation in (a) the proton experiment 7324 and (b) the neutron experiment 7332 [31,32] are shown for LYSO (top), BaF₂ (middle), and PWO crystals (bottom).

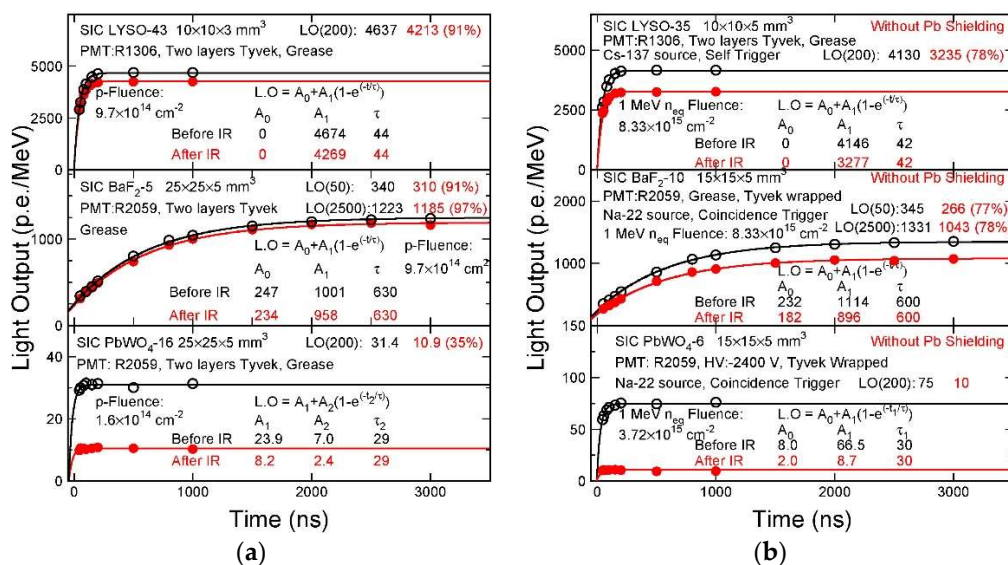


Figure 2. LO measured before (black) and after (red) irradiation in (a) the proton experiment 7324 and (b) the neutron experiment 7332 [31,32] is shown as a function of the integration time for LYSO (top), BaF₂ (middle), and PWO crystals (bottom).

Figure 3 shows the normalized LO integrated in 50 ns gate as a function of the emission-weighted RIAC (EWRIAC) of the 220-nm peak for BaF₂ samples used in (a) the proton experiment 7324 and the neutron experiment 7332 and (b) the neutron experiment 7332 and 7638, respectively. Correlation coefficients of 0.91, 0.95, and 0.95 were observed for 18 BaF₂ plates of 5 mm in Figure 3a, and 12 BaF₂ plates of 15 × 15 × 5 mm³ and 16 BaF₂ plates of 10 × 10 × 2 mm³ in Figure 3b. It is interesting to note that the relative LO loss can be ascribed to the radiation-induced absorption for both proton and neutron irradiation. It is also interesting to note that the mean light path length, which is *L*, shown in these figures, depends on the sample thickness.

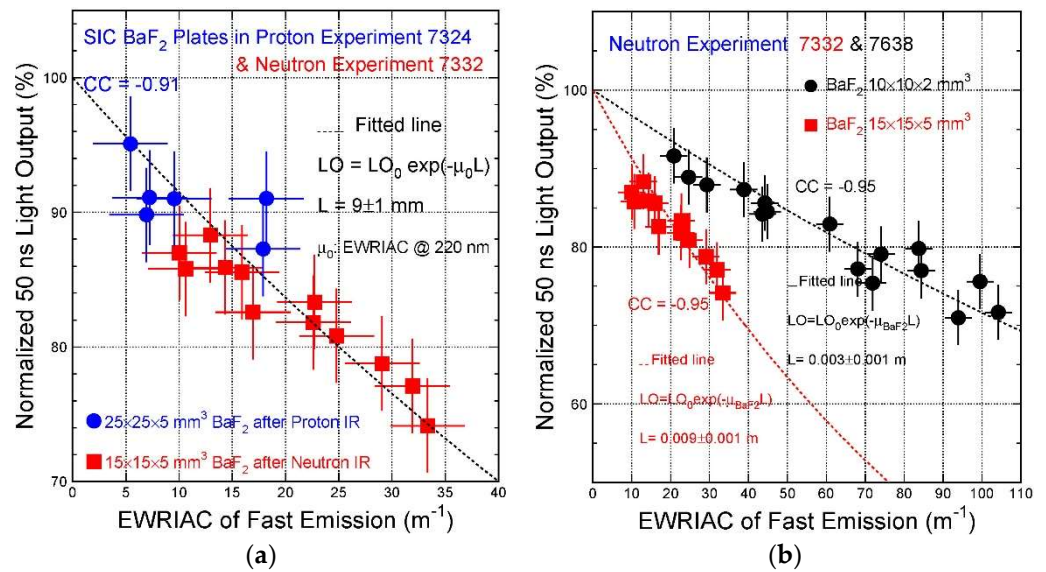


Figure 3. The normalized LO integrated in 50 ns gate is shown as a function of EWRIAC of the 220nm peak for the BaF₂ samples used in (a) the proton experiment 7324 and the neutron experiment 7332 [28], and (b) the neutron experiment 7332 and 7638, respectively.

Figure 4 shows the RIAC values as a function of (a) the proton fluence [25–27,35] and (b) the one MeV equivalent neutron fluence [32] for LYSO/LFS crystals from different vendors irradiated in the proton experiments 6990 and 7324 up to 3.0×10^{15} p/cm² and the proton experiment at CERN PS-IRRAD up to 8.2×10^{15} p/cm² and the neutron experiments 6991, 7332, and 7638 up to 9.2×10^{15} n_{eq}/cm².

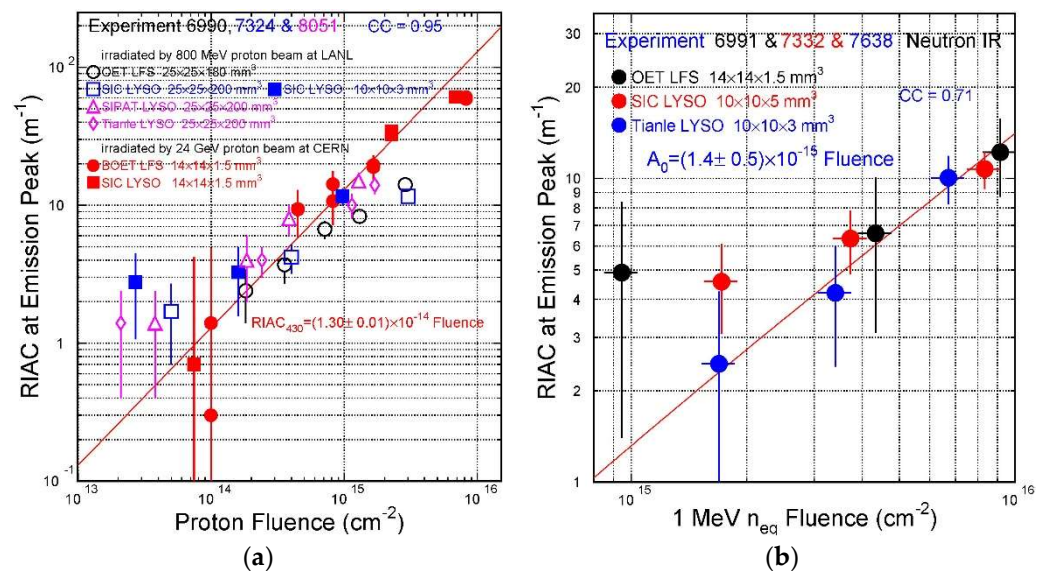


Figure 4. The RIAC values are shown as a function of (a) the proton fluence [25–27,35] and (b) the one MeV equivalent neutron fluence [32] for LYSO/LFS crystals from different vendors irradiated in the proton experiment 6990, 7324 and at the CERN PS-IRRAD experiment and the neutron experiment 6991, 7332, and 7638, respectively.

Also shown in the figure are the corresponding fits and the uncertainties of the fittings, which depend on the uncertainties of the data points. The result also shows a consistent linear relation between the RIAC values at 430 nm and the proton fluence for LYSO crystals from different vendors with a correlation coefficient (CC) of 0.95. The corresponding value

is 0.71 for one MeV equivalent neutron fluence. The radiation hardness specification for the CMS BTL LYSO crystals of $3.12 \times 3.12 \times 57 \text{ mm}^3$ is: RIAC should be less than 3 m^{-1} after 48 kGy, $2.5 \times 10^{13} \text{ p/cm}^2$ and $3 \times 10^{14} \text{ n}_{\text{eq}}/\text{cm}^2$. It is clear that LYSO crystals from different vendors meet the CMS BTL specification.

We also notice that the numerical RIAC values for LYSO against neutrons are a factor of ten less than that against 800 MeV protons at LANSCE and 24 GeV at CERN. This difference can be ascribed to damage by ionization energy loss from protons as compared to damage by displacement and nuclear breakup only from neutrons.

Figure 5 shows RIAC values as a function of (a) proton fluence [33] and (b) one MeV equivalent neutron fluence [33] for LuAG:Ce ceramics, LYSO:Ce, and BaF₂ crystals irradiated in the proton experiment at CERN PS-IRRAD up to $8.2 \times 10^{15} \text{ p/cm}^2$ and the neutron experiment 7638 up to $6.7 \times 10^{15} \text{ n}_{\text{eq}}/\text{cm}^2$, respectively. Also shown are the corresponding fits. It is interesting to note that the RIAC values for LuAG:Ce ceramics are a factor of two smaller than that of LYSO:Ce crystals. This material thus is promising for future colliders with harsh radiation environments, such as the proposed FCC-hh. We also note that large systematic uncertainties were observed for LuAG:Ce ceramics with poor initial transparency. The surface condition of and the scattering centers inside the ceramic bulk may degrade measured transmission and thus introduce a large systematic uncertainty in the RIAC values. The EWLTL values of two ceramic samples shown in Figure 5a, for example, are 67.6% and 32.1% before irradiation and 67.5% and 31.9% after $7.1 \times 10^{13} \text{ p/cm}^2$ and $1.2 \times 10^{15} \text{ p/cm}^2$, respectively, corresponding to RIAC values of 0.5 and 7.1 m^{-1} . Further improvement in optical quality, fast-total ratio (F/T), and radiation hardness of LuAG:Ce ceramics are important for such investigation.

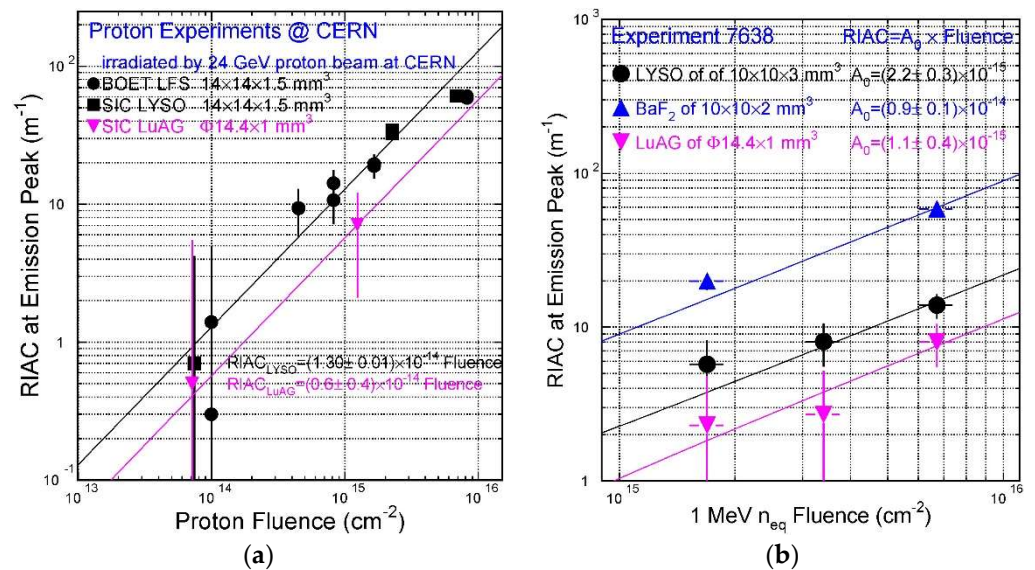


Figure 5. The RIAC values are shown as a function of (a) proton fluence [33] and (b) one MeV equivalent neutron fluence [33] for LuAG:Ce ceramics, LYSO:Ce, and BaF₂ crystals irradiated in the proton experiment at CERN PS-IRRAD and the neutron experiment 7638 at LANSCE, respectively.

Figure 6 shows the LO normalized to before irradiation as a function of (a) proton fluence [28] and (b) one MeV equivalent neutron fluence [32] for LYSO, BaF₂, and PWO plates irradiated in the proton experiment 7324 up to $9.7 \times 10^{14} \text{ p/cm}^2$ and the neutron experiment 7332 up to $8.3 \times 10^{15} \text{ n}_{\text{eq}}/\text{cm}^2$, respectively. It is interesting to note that both LYSO:Ce and BaF₂ plates maintain more than 85% and 75% of light output after a proton fluence of $9.7 \times 10^{14} \text{ p/cm}^2$ and a one-MeV-equivalent neutron fluence of $8.3 \times 10^{15} \text{ n}_{\text{eq}}/\text{cm}^2$. This result indicates that the radiation hardness of BaF₂ is similar to LYSO:Ce under high hadron fluence. BaF₂ crystals, however, have an issue of slow component with a decay time of 600 ns. Yttrium doping in BaF₂ suppresses the slow component effectively while

maintaining the ultrafast light [30,36–40]. An investigation is ongoing to understand hadron-induced radiation damage in BaF₂:Y crystals.

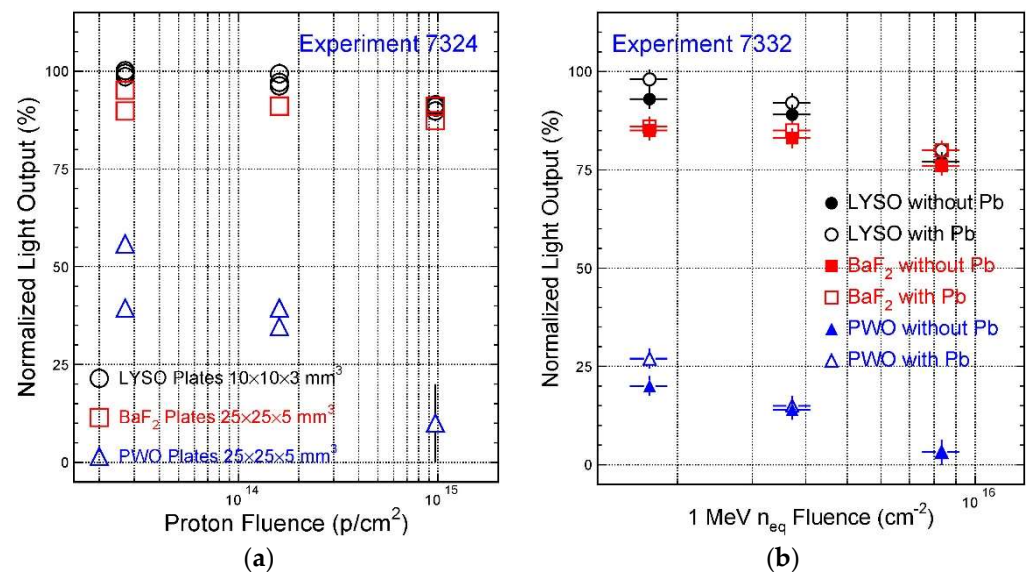


Figure 6. The LO values normalized before irradiation are shown as a function of (a) the proton fluence [28] and (b) the one MeV equivalent neutron fluence [32] for LYSO, BaF₂, and PWO plates irradiated in the proton experiment 7324 and the neutron experiment 7332, respectively.

4. Conclusions

Radiation damage was measured before and after proton and neutron irradiation conducted at LANSCE and CERN for LYSO, BaF₂, and PWO crystals and LuAG ceramics. Both LYSO and BaF₂ plates maintain more than 85% and 75% of light output after proton and neutron irradiation up to 3.0×10^{14} p/cm² and 9.2×10^{15} n_{eq}/cm², respectively. LYSO:Ce and LFS crystals from different vendors show consistent damage against protons of 800 MeV and 24 GeV. The RIAC values for LuAG:Ce ceramics are a factor of two smaller than that of LYSO:Ce crystals against both neutrons and protons. The radiation hardness of BaF₂ is similar to that of LYSO:Ce at high hadron fluence. We plan to improve optical quality, F/T ratio, and radiation hardness for LuAG:Ce and BaF₂:Y crystals. We also plan to investigate radiation damage in various fast and heavy inorganic scintillators against ionization dose, protons, and neutrons.

Author Contributions: Conceptualization, R.-Y.Z.; methodology, R.-Y.Z., L.Z. and R.N.; software, C.H., F.Y., L.Z., R.-Y.Z. and M.M.; investigation, C.H., F.Y., L.Z., R.-Y.Z., X.L. and Z.W.; resources, R.-Y.Z., J.K., R.N., M.M., S.W. and Z.W.; writing—original draft preparation, C.H.; writing—review and editing, L.Z. and R.-Y.Z. All authors have read and agreed to the published version of the manuscript.

Funding: This research was funded by the Department of Energy, Office of Science, Office of High Energy Physics, under award number DE-SC0011925 and DE-AC52-06NA25396.

Data Availability Statement: All data are available on the Web. The data presented in this paper are openly available in: <http://www.hep.caltech.edu/~zhu/> accessed on 9 August 2022.

Acknowledgments: Samples used in this investigation are provided by SIC, BGRI, BOET, SIPAT, SIOM, and Tianle. The authors would like to thank the CERN PS-IRRAD proton facility for providing the 24 GeV proton beams used in this investigation.

Conflicts of Interest: The authors declare no conflict of interest.

References

1. Aleksa, M.; Allport, P.; Bosley, R.; Faltova, J.; Gentil, J.; Goncalo, R.; Helsens, C.; Henriques, A.; Karyukhin, A.; Kieseler, J.; et al. Calorimeters for the FCC-Hh. *arXiv* **2019**, arXiv:1912.09962.
2. Butler, J.N.; Tabarelli de Fatis, T. *A MIP Timing Detector for the CMS Phase-2 Upgrade*; CMS Collaboration: Geneva, Switzerland, 2019.
3. Pezzullo, G.; Budagov, J.; Carosi, R.; Cervelli, F.; Cheng, C.; Cordelli, M.; Corradi, G.; Davydov, Y.; Echenard, B.; Giovannella, S.; et al. The LYSO Crystal Calorimeter for the Mu2e Experiment. *J. Instrum.* **2014**, *9*, C03018. [[CrossRef](#)]
4. Oishi, K. An LYSO Electromagnetic Calorimeter for COMET at J-Park. In *Paper O47-4 Presented in IEEE NSS 2014*; IEEE: Seattle, WA, USA, 2014.
5. Zhang, S.N.; Adriani, O.; Albergo, S.; Ambrosi, G.; An, Q.; Bao, T.W.; Battiston, R.; Bi, X.J.; Cao, Z.; Chai, J.Y.; et al. *The High Energy Cosmic-Radiation Detection (HERD) Facility Onboard China's Space Station*; Takahashi, T., den Herder, J.-W.A., Bautz, M., Eds.; SPIE: Montreal, QC, Canada, 2014; p. 91440X.
6. Anderson, T.; Barbera, T.; Blend, D.; Chigurupati, N.; Cox, B.; Debbins, P.; Dubnowski, M.; Herrmann, M.; Hu, C.; Ford, K.; et al. RADICAL: Precision-Timing, Ultracompact, Radiation-Hard Electromagnetic Calorimetry. *arXiv* **2022**, arXiv:2203.12806. [[CrossRef](#)]
7. Abusalma, F.; Ambrose, D.; Artikov, A.; Bernstein, R.; Blazey, G.C.; Bloise, C.; Boi, S.; Bolton, T.; Bono, J.; Bonventre, R.; et al. Expression of Interest for Evolution of the Mu2e Experiment. *arXiv* **2018**, arXiv:1802.02599.
8. Auffray, E.; Barysevich, A.; Fedorov, A.; Korjik, M.; Koschan, M.; Lucchini, M.; Mechinski, V.; Melcher, C.L.; Voitovich, A. Radiation Damage of LSO Crystals under γ - and 24GeV Protons Irradiation. *Nucl. Instrum. Methods Phys. Res. A* **2013**, *721*, 76–82. [[CrossRef](#)]
9. Derdzian, M.V.; Ovanesyan, K.L.; Petrosyan, A.G.; Belsky, A.; Dujardin, C.; Pedrini, C.; Auffray, E.; Lecoq, P.; Lucchini, M.; Pauwels, K. Radiation Hardness of LuAG:Ce and LuAG:Pr Scintillator Crystals. *J. Cryst. Growth* **2012**, *361*, 212–216. [[CrossRef](#)]
10. Petrosyan, A.G.; Ovanesyan, K.L.; Derdzian, M.V.; Ghambaryan, I.; Patton, G.; Moretti, F.; Auffray, E.; Lecoq, P.; Lucchini, M.; Pauwels, K.; et al. A Study of Radiation Effects on LuAG:Ce(Pr) Co-Activated with Ca. *J. Cryst. Growth* **2015**, *430*, 46–51. [[CrossRef](#)]
11. Shen, Y.; Feng, X.; Shi, Y.; Vedda, A.; Moretti, F.; Hu, C.; Liu, S.; Pan, Y.; Kou, H.; Wu, L. The Radiation Hardness of Pr:LuAG Scintillating Ceramics. *Ceram. Int.* **2014**, *40*, 3715–3719. [[CrossRef](#)]
12. Dissertori, G.; Luckey, D.; Nessi-Tedaldi, F.; Pauss, F.; Wallny, R. Performance Studies of Scintillating Ceramic Samples Exposed to Ionizing Radiation. In *Proceedings of the 2012 IEEE Nuclear Science Symposium and Medical Imaging Conference Record (NSS/MIC)*, Anaheim, CA, USA, 29 October–3 November 2012; pp. 305–307.
13. Dormenev, V.; Korjik, M.; Kuske, T.; Mechinski, V.; Novotny, R.W. Comparison of Radiation Damage Effects in PWO Crystals Under 150 MeV and 24 GeV High Fluence Proton Irradiation. *IEEE Trans. Nucl. Sci.* **2014**, *61*, 501–506. [[CrossRef](#)]
14. The CMS Electromagnetic Calorimeter Group; Adzic, P.; Almeida, N.; Andelin, D.; Anicin, I.; Antunovic, Z.; Arcidiacono, R.; Arenton, M.W.; Auffray, E.; Argiro, S.; et al. Radiation Hardness Qualification of PbWO₄ Scintillation Crystals for the CMS Electromagnetic Calorimeter. *J. Instrum.* **2010**, *5*, P03010. [[CrossRef](#)]
15. Dissertori, G.; Perez, C.M.; Nessi-Tedaldi, F. A FLUKA Study towards Predicting Hadron-Specific Damage Due to High-Energy Hadrons in Inorganic Crystals for Calorimetry. *J. Instrum.* **2020**, *15*, P06006. [[CrossRef](#)]
16. Dissertori, G.; Luckey, D.; Nessi-Tedaldi, F.; Pauss, F.; Quittnat, M.; Wallny, R.; Glaser, M. Results on Damage Induced by High-Energy Protons in LYSO Calorimeter Crystals. *Nucl. Instrum. Methods Phys. Res. A* **2014**, *745*, 1–6. [[CrossRef](#)]
17. Dissertori, G.; Lecomte, P.; Luckey, D.; Nessi-Tedaldi, F.; Pauss, F.; Otto, Th.; Roesler, S.; Urscheler, Ch. A Study of High-Energy Proton Induced Damage in Cerium Fluoride in Comparison with Measurements in Lead Tungstate Calorimeter Crystals. *Nucl. Instrum. Methods Phys. Res. A* **2010**, *622*, 41–48. [[CrossRef](#)]
18. Lucchini, M.T.; Pauwels, K.; Blazek, K.; Ochesanu, S.; Auffray, E. Radiation Tolerance of LuAG:Ce and YAG:Ce Crystals Under High Levels of Gamma- and Proton-Irradiation. *IEEE Trans. Nucl. Sci.* **2016**, *63*, 586–590. [[CrossRef](#)]
19. Nessi-Tedaldi, F. Studies of the Effect of Charged Hadrons on Lead Tungstate Crystals. *J. Phys. Conf. Ser.* **2009**, *160*, 012013. [[CrossRef](#)]
20. Dissertori, G.; Luckey, D.; Nessi-Tedaldi, F.; Pauss, F.; Wallny, R.; Spikings, R.; van der Lelij, R.; Arnau Izquierdo, G. A Visualization of the Damage in Lead Tungstate Calorimeter Crystals after Exposure to High-Energy Hadrons. *Nucl. Instrum. Methods Phys. Res. A* **2012**, *684*, 57–62. [[CrossRef](#)]
21. Lecomte, P.; Luckey, D.; Nessi-Tedaldi, F.; Pauss, F. High-Energy Proton Induced Damage Study of Scintillation Light Output from Calorimeter Crystals. *Nucl. Instrum. Methods Phys. Res. A* **2006**, *564*, 164–168. [[CrossRef](#)]
22. Huhtinen, M.; Lecomte, P.; Luckey, D.; Nessi-Tedaldi, F.; Pauss, F. High-Energy Proton Induced Damage in PbWO₄ Calorimeter Crystals. *Nucl. Instrum. Methods Phys. Res. A* **2005**, *545*, 63–87. [[CrossRef](#)]
23. Auffray, E.; Korjik, M.; Singovski, A. Experimental Study of Lead Tungstate Scintillator Proton-Induced Damage and Recovery. *IEEE Trans. Nucl. Sci.* **2012**, *59*, 2219–2223. [[CrossRef](#)]
24. Batarin, V.A.; Brennan, T.; Butler, J.; Cheung, H.; Datsko, V.S.; Davidenko, A.M.; Derevschikov, A.A.; Dzhelyadin, R.I.; Fomin, Y.V.; Frolov, V.; et al. Study of Radiation Damage in Lead Tungstate Crystals Using Intense High-Energy Beams. *Nucl. Instrum. Methods Phys. Res. A* **2003**, *512*, 488–505. [[CrossRef](#)]
25. Yang, F.; Zhang, L.; Zhu, R.-Y.; Kapustinsky, J.; Nelson, R.; Wang, Z. Proton Induced Radiation Damage in Fast Crystal Scintillators. *Nucl. Instrum. Methods Phys. Res. A* **2016**, *824*, 726–728. [[CrossRef](#)]

26. Yang, F.; Zhang, L.; Zhu, R.-Y.; Kapustinsky, J.; Nelson, R.; Wang, Z. Proton-Induced Radiation Damage in Fast Crystal Scintillators. *IEEE Trans. Nucl. Sci.* **2017**, *64*, 665–672. [[CrossRef](#)]
27. Yang, F.; Zhang, L.; Zhu, R.-Y.; Kapustinsky, J.; Nelson, R.; Wang, Z. Proton-Induced Radiation Damage in BGO, LFS, PWO and a LFS/W/Quartz Capillary Shashlik Cell. In Proceedings of the 2016 IEEE Nuclear Science Symposium, Medical Imaging Conference and Room-Temperature Semiconductor Detector Workshop (NSS/MIC/RTSD), Strasbourg, France, 29 October–6 November 2016; pp. 1–4.
28. Hu, C.; Yang, F.; Zhang, L.; Zhu, R.-Y.; Kapustinsky, J.; Nelson, R.; Wang, Z. Proton-Induced Radiation Damage in BaF₂, LYSO, and PWO Crystal Scintillators. *IEEE Trans. Nucl. Sci.* **2018**, *65*, 1018–1024. [[CrossRef](#)]
29. Chipaux, R.; Borizevich, A.; Dujardin, C.; Lecocq, P.; Korzhik, M.V. Behaviour of PWO Scintillators after High Fluence Neutron Irradiation. In Proceedings of the 8th International Conference on Inorganic Scintillators and Their Applications, Alushta, Ukraine, 19–23 September 2005; pp. 369–371.
30. Baranov, V.; Davydov, Y.I.; Vasilyev, I.I. Light Outputs of Yttrium Doped BaF₂ Crystals Irradiated with Neutrons. *J. Instrum.* **2022**, *17*, P01036. [[CrossRef](#)]
31. Hu, C.; Yang, F.; Zhang, L.; Zhu, R.-Y.; Kapustinsky, J.; Mocko, M.; Nelson, R.; Wang, Z. Neutron-Induced Radiation Damage in BaF₂, LYSO/LFS and PWO Crystals. *J. Phys. Conf. Ser.* **2019**, *1162*, 012020. [[CrossRef](#)]
32. Hu, C.; Yang, F.; Zhang, L.; Zhu, R.-Y.; Kapustinsky, J.; Mocko, M.; Nelson, R.; Wang, Z. Neutron-Induced Radiation Damage in LYSO, BaF₂, and PWO Crystals. *IEEE Trans. Nucl. Sci.* **2020**, *67*, 1086–1092. [[CrossRef](#)]
33. Hu, C.; Zhang, L.; Zhu, R.-Y.; Li, J.; Jiang, B.; Kapustinsky, J.; Mocko, M.; Nelson, R.; Li, X.; Wang, Z. Hadron-Induced Radiation Damage in LuAG:Ce Scintillating Ceramics. *IEEE Trans. Nucl. Sci.* **2022**, *69*, 181–186. [[CrossRef](#)]
34. Ma, D.; Zhu, R. Light Attenuation Length of Barium Fluoride Crystals. *Nucl. Instrum. Methods Phys. Res. A* **1993**, *333*, 422–424. [[CrossRef](#)]
35. Yang, F.; Zhang, L.; Zhu, R.-Y. Gamma-Ray Induced Radiation Damage Up to 340 Mrad in Various Scintillation Crystals. *IEEE Trans. Nucl. Sci.* **2016**, *63*, 612–619. [[CrossRef](#)]
36. Sobolev, B.P.; Krivandina, E.A.; Derenzo, S.E.; Moses, W.W.; West, A.C. Suppression of BaF₂ Slow Component of X-RAY Luminescence in Non-Stoichiometric Ba_{0.9}R_{0.1}F_{2.1} Crystals (R = Rare Earth Element). *MRS Proc.* **1994**, *348*, 277. [[CrossRef](#)]
37. Radzhabov, E.; Istomin, A.; Nepomnyashikh, A.; Egranov, A.; Ivashchkin, V. Exciton Interaction with Impurity in Barium Fluoride Crystals. *Nucl. Instrum. Methods Phys. Res. A* **2005**, *537*, 71–75. [[CrossRef](#)]
38. Myasnikova, A.S.; Radzhabov, E.A.; Egranov, A.v. Extrinsic Luminescence of BaF₂:R³⁺ Crystals (R³⁺ = La³⁺, Y³⁺, Yb³⁺). *Phys. Solid State* **2008**, *50*, 1644–1647. [[CrossRef](#)]
39. Chen, J.; Yang, F.; Zhang, L.; Zhu, R.-Y.; Du, Y.; Wang, S.; Sun, S.; Li, X. Slow Scintillation Suppression in Yttrium Doped BaF₂ Crystals. *IEEE Trans. Nucl. Sci.* **2018**, *65*, 2147–2151. [[CrossRef](#)]
40. Gundacker, S.; Pots, R.H.; Nepomnyashchikh, A.; Radzhabov, E.; Shendrik, R.; Omelkov, S.; Kirm, M.; Acerbi, F.; Capasso, M.; Paternoster, G.; et al. Vacuum Ultraviolet Silicon Photomultipliers Applied to BaF₂ Cross-Luminescence Detection for High-Rate Ultrafast Timing Applications. *Phys. Med. Biol.* **2021**, *66*, 114002. [[CrossRef](#)] [[PubMed](#)]